A simplified variational analysis scheme for soil moisture: Developments at Météo-France and MSC

G. Balsamo[1], F. Bouyssel[2], J. Noilhan[2], J.-F. Mahfouf[1], S. Bélair[1] and G. Deblonde[1]

[1]*Meteorological Service of Canada, MRB/RPN*
2121 Trans-Canada Highway, Dorval, PQ, H9P 1J3, CANADA
[2]*Météo-France/CNRM*
42, Av. G. Coriolis, 31057 Toulouse, FRANCE

ABSTRACT

A simplified variational data assimilation technique, developed for the land surface initialization of a numerical weather prediction (NWP) model, is considered in the frame of the ELDAS project at Météo-France, for the production of a daily soil moisture over Europe. The assimilation of indirect data of screen-level temperature and relative humidity is combined with a complementary correction based on precipitation error. The simplified variational approach obtains the linearized observation operator from perturbed integration(s) of the NWP model. The linearity of the observation operator and the horizontal decoupling between grid points allow the simplified 2D-VAR formalism, applied on each grid point separately. The corrections applied to the soil moisture field are adapted to the current meteorological conditions and the grid point characteristics (texture and vegetation), as well as to the previous soil state. The complementary correction based on precipitation error is applied with an optimum interpolation (OI) approach. The results obtained within ELDAS at Météo-France are presented and discussed.
The assimilation of other sources of data is investigated, with an Observing System Simulated Experiment (OSSE) conducted at the Meteorological Service of Canada. The assimilation of current available satellite observations provided by AQUA satellite (microwave C-band), GOES (infrared), and the potential of observations provided in the future by SMOS and HYDROS satellite missions (microwave L-band) is investigated. The results of this study are presented and perspectives are provided.

1 Introduction

Continental soil moisture plays an important role in near surface and tropospheric processes and therefore it has received considerable attention by the Numerical Weather Prediction (NWP) and Climate research community in recent years (Koster et al., 2004). Furthermore it is a key variable for hydrological and agricultural modelling applications, supporting the management of many human activities, including floods and droughts risks assessment. The atmospheric impact of soil water content comes via the partitioning of latent and sensible heat fluxes at the surface. A direct measure of soil moisture is difficult and no extensive observation network presently exists. In addition, site measurements have the problem of representativity (Kerr et al. 2001), due to the low spatial correlation of soil moisture associated to the land surface heterogeneity. For these reasons, the assimilation of indirect observations from ground-based (raingauges, radars, screen-level) and satellite instruments (infrared and microwave radiometers) has been studied for the analysis of soil moisture. In particular, the assimilation of screen-level temperature and relative humidity observations with the optimum interpolation (OI) technique (Mahfouf 1991, Bouttier et al. 1993 I,II) has proven to be reliable to retrieve the soil water content under specific meteorological conditions, and is currently used in operations in different NWP centres (Giard and Bazile 2000, Mahfouf et al. 2000, Bélair et al. 2003 I,II). In recent years, several studies have focused on the variational technique for the analysis of soil moisture via the assimilation of screen-level observations, as first examined by Mahfouf (1991), showing the reliability for operational NWP : Callies et al. (1998), Rhodin et al. (1999), Bouyssel et al. (2000), Hess (2001), Seuffert et al. (2004), and Balsamo et al. (2004).

In the present work, the analysis of total soil water content is developed in an operational NWP context. A bi-dimensional simplified variational analysis (2D-VAR), based on a linear estimate of the observation operator, is developed, and tested in the European Land Data Assimilation System (ELDAS, van den Hurk, 2002). The NWP models, the land surface parameterization and the simplified 2D-VAR soil moisture analysis are presented. The potential of other observation types is investigated at the Meteorological Service of Canada (MSC) in a Observing System Simulated Experiment (OSSE). A set of simulated observations is generated and assimilated in a Canadian Land Data Assimilation System (CaLDAS) prototype. The influence matrix diagnostics (Cardinali et al., 2003) provide the information content of the observations in the analysis allowing to put into perspective the importance of each source of observation in correcting a prescribed soil moisture error.

2 Model and assimilation description at Météo-France

2.1 The atmospheric models

The limited area NWP model ALADIN (Bubnová et al. 1993) and the ARPEGE global model (Courtier et al. 1991) are used in this study. The two models have the same physical and dynamical cores, and both are used operationally at Météo-France for short-range weather forecasting. The ALADIN version in this study has 31 vertical levels and a horizontal grid size of 9.92 km. The ARPEGE version has 41 vertical levels and a Gaussian variable grid size ranging from 20 km over France (pole) to 200 km on the Pacific Ocean (anti-pole). A two time-level semi-Lagrangian semi-implicit advection scheme is used. The horizontal diffusion is a spectral fourth-order scheme. The physical parameterizations are described in Geleyn et al. (1995). In particular, atmospheric turbulent exchange-coefficients for heat and momentum are described in Louis (1979) and Louis et al. (1981). The estimation of screen-level parameters is provided by a vertical interpolation between the surface and the lowest atmospheric model layer (Geleyn 1988). A global-scale data assimilation is performed for the analysis of ARPEGE model with 4D-VAR (Janisková et al., 1999) for the atmosphere and OI for the surface. The analyzed fields of ARPEGE are interpolated onto the limited-area domain for the initialization of ALADIN.

2.2 The land surface scheme

The land surface scheme ISBA (Interaction Soil Biosphere Atmosphere) is described in Noilhan and Planton (1989), Noilhan and Mahfouf (1996). It comprises two soil layers with associated variables to describe the evolution of temperature and water content, based on a force-restore mechanism. The operational implementation of the ISBA scheme with a surface analysis, described in Giard and Bazile (2000), has required some further refinements, like the inclusion of soil freezing that allows a better description of the diurnal cycle during winter. The operational version of ISBA describes the evolution of eight prognostic variables: T_s the surface temperature, T_p the mean surface temperature, W_s and W_{si}, the superficial water contents (liquid and ice phase respectively), W_p and W_{pi} the total water contents (liquid and ice phase), W_l the vegetation intercepted water content, and S_n the snow water content. The variables T_s, T_p, W_s, and W_p are operationally analyzed on the global scale by the OI method. Each grid box over land is divided into bare ground and vegetated areas. A single heat budget is considered for the ground and vegetation, and if appropriate, snow cover. Within the hydrological soil reservoir, with a variable depth d_p, a thin top layer ($d_s = 10^{-2}m$) is considered. The soil water can be released into the atmosphere as water vapour by means of the evaporation processes from bare ground and vegetation interception reservoirs, and transpiration of the leaves. The evaporation is assumed to be at the potential rate above the field capacity (w_{fc}), while the transpiration is negligible below the wilting point (w_{wilt}). The soil wetness index SWI, defined as

$$SWI = \frac{(w_p - w_{wilt})}{(w_{fc} - w_{wilt})} \tag{1}$$

is often used alternatively to represent the soil moisture availability for transpiration. In the parameterization of evaporation processes, the superficial water content (W_s) and the total soil water content (W_p) largely determine the evaporation from bare ground and vegetation respectively. W_p depends on the formulation of the stomatal resistance (R_s) which describes the vegetation phenological control on transpiration, while W_s interacts via the surface relative humidity (h_u). Due to the large water storage of the total reservoir, the evolution of W_p during atmospheric forecasts is rather slow, hence its initialization is of crucial importance. An erroneous estimate of the total soil moisture, in fact, affects the quality of the forecast for several days, while an incorrect superficial soil moisture has a shorter impact, typically 1 day long, since it is restored by the total soil moisture and the atmospheric forcing (Bouyssel et al., 2000). Several improved versions of the ISBA scheme have been developed and are used for research studies, including a sub-root zone layer (Boone et al. 1999), a three-layer snow parameterization (Boone and Etchevers 2001), and an interactive vegetation module (Calvet et al. 1998). A sub-grid surface runoff is implemented in a hydrological coupling system ISBA-MODCOU (Habets et al. 1999 I,II).

2.3 The land surface analysis scheme

The land surface analysis scheme, as described in Mahfouf (1991), optimally combines the information provided by screen-level observations and a model forecast (the background term). In the variational method, the optimal weighting of these two components is achieved by the minimisation of a cost function J, which is of the form

$$J(\mathbf{x}) = \frac{1}{2}(\mathbf{x}-\mathbf{x}^b)^T\mathbf{B}^{-1}(\mathbf{x}-\mathbf{x}^b) + \frac{1}{2}(\mathbf{y}-H(\mathbf{x}))^T\mathbf{R}^{-1}(\mathbf{y}-H(\mathbf{x})) \tag{2}$$

where $\mathbf{x}$ is the vector containing the variables to analyze, $\mathbf{x}^b$ is the background state and $\mathbf{y}$ is the observations vector. $\mathbf{B}$ and $\mathbf{R}$ are, respectively, the background and the observation error covariance matrices, and H is the observation operator, that maps the model state vector $\mathbf{x}$ into observation space, including the interpolation in space and integration in time. Under the Tangent Linear (TL) hypothesis, the H operator can be expressed by its first order Taylor expansion

$$H(\mathbf{x}+\delta\mathbf{x}) = H(\mathbf{x}) + \mathbf{H}\delta\mathbf{x} \tag{3}$$

where $\mathbf{H}$ is the TL observation operator matrix; the cost function is then quadratic. The minimization of $J(\mathbf{x})$ is generally an iterative process that makes use of the tangent linear and adjoint models to evaluate the cost function and its gradient. However, for low dimension problems and under the linearity assumption, the minimum of the cost function imposed by $\nabla J(\mathbf{x}) = 0$ can be directly obtained. The $\mathbf{H}$ matrix is evaluated with a finite difference approach, and the analyzed state $\mathbf{x}^a$ is given by the expression

$$\mathbf{x}^a = \mathbf{x}^b + \mathbf{K}(\mathbf{y}-H(\mathbf{x}^b)) \tag{4}$$

where the terms :

$$\mathbf{K} = (\mathbf{B}^{-1}+\mathbf{H}^T\mathbf{R}^{-1}\mathbf{H})^{-1}\mathbf{H}^T\mathbf{R}^{-1} \qquad \text{and} \qquad (\mathbf{y}-H(\mathbf{x}^b)) \tag{5}$$

are respectively named the gain matrix and the innovation vector (difference between the observation and the model forecast in observation space). The linear hypothesis, expressed by Eq.3, is best satisfied in the vicinity of $\mathbf{x}^b$ when corrections to the first guess are small. In the case of the total soil water content (W_p) in ISBA, this algebraic constraint is compatible with the physical behavior of the control variable which evolves with a time-scale of several days.

In the variational analysis of the total soil water content, the linear hypothesis produces an important simplification (hence a *simplified* 2D-VAR) that makes it similar to the OI technique. Both methods in fact obtain the analysis increments directly from Eq. 4, but in the simplified 2D-VAR a dynamical estimate of the gain matrix replaces a statistical evaluation. The application within ELDAS considers the assimilation of the screen-level observations of temperature and relative humidity. The simplified variational assimilation is extended to other relevant satellite observations in its application at the MSC. The observations have been spatially interpolated on the model grid by a previous analysis. In the 2D-VAR method, the atmospheric forcing and the characteristics for soil and vegetation are implicitly taken into account providing analysis increments adapted to the specific time and grid point location without any empirical regression and not limited to the use of observations at a single time.

2.4 The simplified 2D-VAR for W_p analysis

The set up for the simplified 2D-VAR makes use of the full NWP model to infer the 2m forecast sensitivity to soil moisture variations providing a linear estimate of the observation operator (**H**) from which the analysis gain matrix (**K**) is calculated. Let us consider the model guess G and a perturbed state G' where W_p has been modified by a small quantity δW_p, at time t_0. The model integrations starting from the two initial states, G and G', provide the 2m forecast sensitivity evaluated at time t_1 (at which the observations are available):

$$\delta T_{2m}^{(1)} = T_{2m}^{G'(1)} - T_{2m}^{G(1)} \qquad \delta RH_{2m}^{(1)} = RH_{2m}^{G'(1)} - RH_{2m}^{G(1)} \tag{6}$$

Now, considering a 6-h assimilation time-window, the matrices **B**, **R**, $\mathbf{H}^T$, needed for the direct computation of **K** are simply

$$\mathbf{B} = \begin{pmatrix} \sigma_{W_p}^2 \end{pmatrix} \qquad \mathbf{R} = \begin{pmatrix} \sigma_{T_{2m}}^2 & 0 \\ 0 & \sigma_{RH_{2m}}^2 \end{pmatrix} \qquad \mathbf{H}^T = \begin{pmatrix} \frac{\delta T_{2m}^{(1)}}{\delta W_p^{(0)}} \\ \frac{\delta RH_{2m}^{(1)}}{\delta W_p^{(0)}} \end{pmatrix}$$

The correlations between observation errors on T_{2m} and RH_{2m} (off diagonal terms of the **R** matrix), are set to 0. The analysis for W_p, according to Eq. 4, is obtained as follow

$$W_p^a = W_p^b + \begin{pmatrix} k_1 & k_2 \end{pmatrix} \begin{pmatrix} \Delta T_{2m}^{(1)} \\ \Delta RH_{2m}^{(1)} \end{pmatrix} \tag{7}$$

where k_1, k_2 are the elements of the gain matrix; $\Delta T_{2m}^{(1)}$ and $\Delta RH_{2m}^{(1)}$ are elements of the innovation vector. The latter are calculated as differences between the 2m observations and the background, evaluated on the model grid point at time $t_1 = t_0 + 6h$ (at the end of the assimilation time-window). With a 24-h assimilation time-window the soil moisture analysis is performed at 00 UTC and the observations available at 4 synoptic hours (06, 12, 18, 00(day+1) UTC) are assimilated.

For satellite observations (i.e. the microwave brightness temperature at given P polarization, T_b^P, or the clear-sky infra-red skin temperature, T_s^{IR}), the assimilation system has to be capable to ingest observations at any time of day. The number of observations may vary according to the satellite overpasses, the meteorological conditions (in case of T_s^{IR}), and the land surface state.

This method is therefore more flexible than the OI technique, currently designed to assimilate T_{2m} and RH_{2m} every 6 hours.

2.5 The underlying hypotheses

The simplified 2D-VAR method relies on the linear hypothesis of the observation operator, on the horizontal decoupling hypothesis of the soil/screen-level relation, and on the control variable decoupling assumption, allowing to consider the analysis of soil moisture separately from other model variables. These hypotheses allow this 2D formalism to be performed at each grid point separately. Although the linear response of land surface evaporation to a small soil moisture variation is well satisfied, the estimation of the H operator by means of a perturbed forecast may lead to undesired results under specific meteorological conditions. An extensive treatment and validation of those hypotheses are given in Balsamo et al. (2004) in the case of screen-level observations. The optimal set up of the simplified 2D-VAR soil moisture analysis considers a double estimate of the observation operator using 2 opposite phase chess-type initial perturbations. This configuration is preferred to a single estimate of the **H** matrix as it provides a more accurate evaluation without any empirical masking of the analysis (meteorological and surface conditions where **K** is set to 0).

2.6 Evaluation of the analysis convergence

The convergence of the analysis is assessed by assimilating simulated observations. An ALADIN model run initialized with a reference state of soil moisture ($W_p{}^{ref}$ defined for a value of $SWI = 0.5$) provides the simulated observations. The analysis error is evaluated with respect to the reference in terms of root-mean-square error. The convergence towards the reference is checked from an operational analysis (13th June 2000) which provides a wide range of soil moisture states. A realistic set of observation error statistics is adopted ($\sigma^a_{T2m} = 1$K,

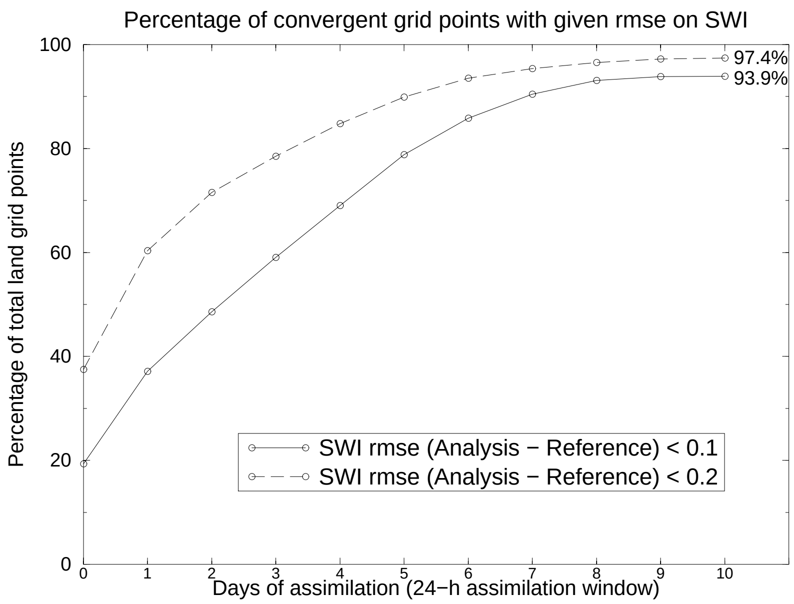

Figure 1: Convergence of 2D-VAR towards $W_p{}^{ref}$. Sequential assimilation with 24-h time-window (simulated observations every 6-h) starting the 13th June 2000. Percentage of total land grid points converging with given rmse on SWI; continuous line: rmse < 0.1, dashed line: rmse < 0.2.

$\sigma^a_{RH2m} = 10\%$), while the background error is inflated (by a factor 2 compared to the value used in the real observation experiments), to obtain a faster convergence ($\sigma^b_{W_p}$=10% $\cdot\,(w_{fc} - w_{wilt})$) and to compensate for the arbitrary choice of the reference state. The simplified 2D-VAR is applied sequentially with a 24-h time-window and observations are assimilated every 6 hours. The observations are generated from the reference run at each cycle without noise ("perfect" observations). The result shows a good convergence after 10 days as illustrated in Figure 1. A 6-h assimilation window has been evaluated showing a similar behavior. This test confirms the convergence of the method for most land grid points ($> 97\%$).

2.7 Assimilation of real observations

Two distinct 2D-VAR assimilation experiments are done over 25 days from the 4th to the 28th of June 2000, using a 6-h and a 24-h assimilation time-window. Both experiments start from an initial soil moisture set to

$W_p{}^{ref}$ ($SWI = 0.5$) and an equal setting of the error statistics ($\sigma^o_{T2m} = 1$K, $\sigma^o_{RH2m} = 10\%$ and $\sigma^b_{W_p}$=5% $\cdot (w_{fc} - w_{wilt})$. The operational atmospheric analysis from ARPEGE prescribes the initial and boundary conditions for the atmospheric fields (no atmospheric assimilation is re-performed), while the OI land surface analysis scheme is applied to T_s, T_p, and W_s (the 2D-VAR is applied to W_p only). The choice of a uniform initial state allows to study the horizontal gradients of soil moisture generated during the assimilation cycles. The soil moisture reaches a complex and realistic structure after a few days of assimilation as shown in Figure2 (after 12 days). The soil moisture field produced over France with the ISBA-MODCOU off-line system, driven by analyzed atmospheric forcing for precipitation and radiation (Habets et al. 1999 I,II), is considered as accurate product for evaluation. The soil moisture fields obtained from the 2D-VAR analyses with different assimilation windows, show common large scale structures. The signal on the Alpine region, the Central Massif and the Pyrenees are comparable to the off-line ISBA-MODCOU field (Figure 4).

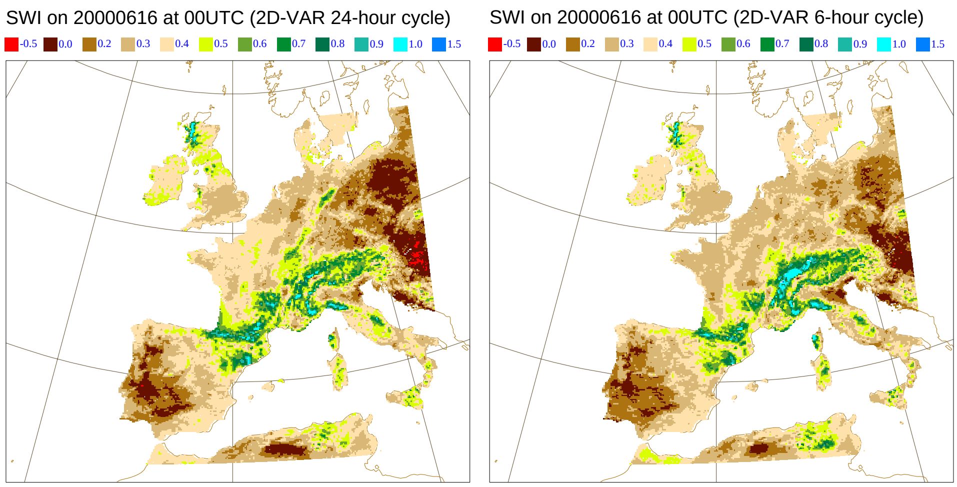

Figure 2: Example of total soil moisture initialization (SWI): assimilation tests using 2D-VAR analysis with a 24-h (left panel) and a 6-h (right panel) assimilation time-window, after 12 days of assimilation.

An objective validation is done by computating forecast scores and comparing the simplified 2D-VAR to the operational (OI). The 2m forecast scores for temperature and relative humidity are calculated during the whole period. A set of 72-hour forecasts starting at 00 UTC is performed. The scores provide a robust test as the observations come from about 1500 synoptic stations over Europe. Although the main soil moisture structures are similar (Figure 2), better objective scores are obtained for the longer assimilation window (24-h) in accordance with thoretical expectations. The introduction of the new soil moisture analysis shows a clear improvement of the 2m forecast with respect to the operational OI analysis (both in BIAS and RMSE). This result is particularly significant if combined with the achievement of a more realistic field of soil moisture.

3 The ELDAS set-up at Météo-France

The ELDAS set-up at Météo-France considers the use of a NWP model for the assimilation cycle. The simplified 2D-VAR with a 24-h assimilation is applied to the total soil moisture, while the OI analysis (Giard and Bazile, 2000) provides the initialization for soil temperature and surface soil moisture. The ARPEGE global model, operational at Météo-France, performs the integrations useful for the assimilation cycle. A Gaussian grid mesh with a stretching factor of 3.5, allows for a finer resolution over the ELDAS domain. The ECOCLIMAP physiography database (Masson et al., 2003) including the FAO98 Soil texture database is implemented. The ECOCLIMAP database is extracted at a 0.08° resolution and interpolated onto the ARPEGE grid. The physiography obtained is considered as a reference in the ELDAS experiment. The simplified variational soil moisture analysis (Balsamo et al., 2004), developed for the ALADIN LAM model, has been adapted for the ARPEGE

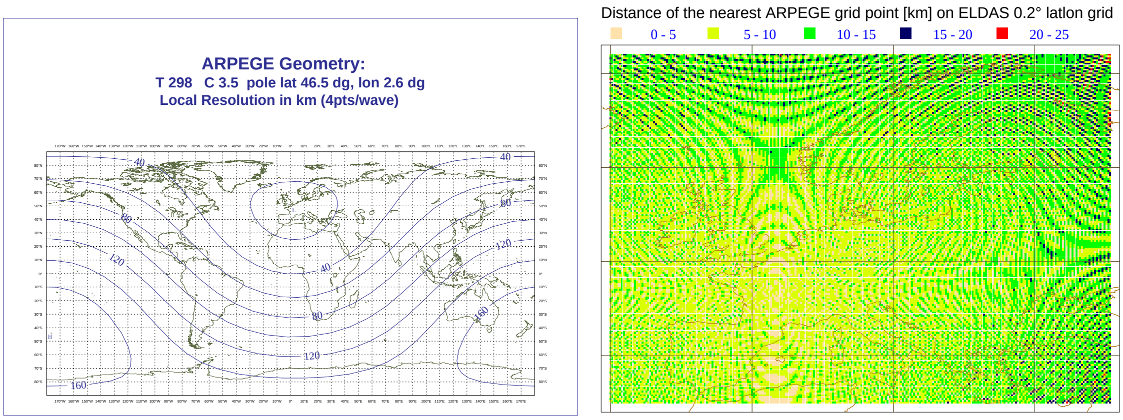

Figure 3: ARPEGE horizontal resolution (left panel) and distance of the nearest ARPEGE grid point on the ELDAS output grid (right panel).

global analysis. The treatment of atmospheric fields during the assimilation cycle (atmospheric blending) and the use of ELDAS precipitation forcing to provide an external correction to soil moisture are illustrated in the following section.

3.1 The atmospheric blending

The ELDAS experiment can be regarded as a surface re-analysis, where the land surface is readjusted according to a different physiography, data assimilation method, and external forcing. In order to preserve the atmospheric feedback of a new land surface during the assimilation cycle without performing a full atmospheric reanalysis, a blending technique (Guidard and Fischer, 2003) has been implemented. This technique aims at combining the ”large scales” resolved by previously archived ARPEGE analyses with new ”mesoscale” features provided by the short-range forecasts which include the land surface modifications (soil variables state and ancillary data). This allows one to build a new atmospheric analysis field without direct use of upper-air observations which would imply to re-run an atmospheric 4D-VAR. Blending of spectral atmospheric fields is done at two different truncations: T161 for the large scales and T298 (full ARPEGE model resolution) for the small scales.

The atmospheric blended state is computed as

$$ARP_{Blended} = ARP_A + [ARP_G - ARP_A]_{highres} \tag{8}$$

where ARP_A, the archive ARPEGE analysis, is kept integrally for the large-scale features, and the information brought by the new guess ARP_G is added for the mesoscale features. The surface fields are taken from the new OI/2D-VAR land surface analysis. For the production of ELDAS fields, an interpolation technique based on the nearest grid point is used to map the ARPEGE grid to the ELDAS grid. The working grid domain within the assimilation cycle is the ARPEGE grid, while the output domain is the ELDAS grid. The nearest grid point interpolation technique is used for the mapping from/to the defined working/output grid domains, and applies to ancillary data, forecast, forcing, analysis, and data exchange. This choice avoids the loss of the original values of the fields (with only a geolocalization error due to the distance between ELDAS and ARPEGE grid points, estimated in Figure 3). The self-consistency of the output fields is preserved, although the accuracy of the method in case of complex terrain (i.e. steep orography) could be questionable.

3.2 A 6-month assimilation cycle

The ELDAS data assimilation cycle has been integrated for a 6-month period starting 1st May 2000. This long integration allows one to obtain an equilibrium in the land surface state. For illustration purposes, the output of the ARPEGE 2D-VAR cycle, extracted for the 00 UTC 16th June 2000, is compared with that of the ISBA-MODCOU soil moisture in Figure 4.

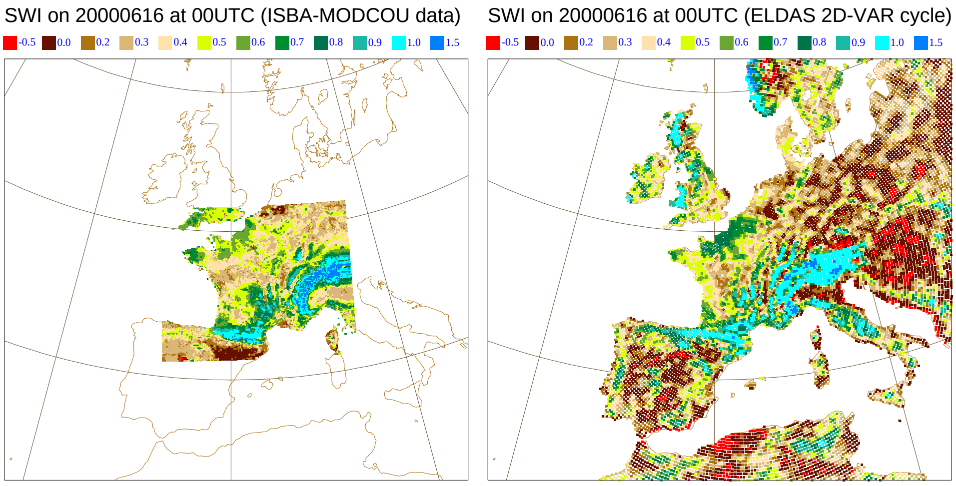

Figure 4: Total soil moisture initialization (SWI): Comparison of the Off-line ISBA-MODCOU (left panel) and the ELDAS 2D-VAR analysis with a 24-h (right panel) obtained with the ARPEGE model.

The comparison of the total soil water content field over France shows an improved match of humid and dry patterns with respect to previous results (Figure 2). The main reasons for such an improvement are related to the use of a consistent ancillary dataset (ECOCLIMAP in both cases), and to a longer data assimilation cycle with respect to the ALADIN experiment.

3.3 The use of precipitation forcing

The use of ELDAS 24-hour accumulated precipitation analyses is investigated for applying a complementary correction to the soil moisture fields. The analyzed ELDAS precipitation forcing is provided by the University of Vienna (Rubel et al. 2004). The output data is on the ELDAS 0.2° regular grid and is interpolated onto the ARPEGE grid to calculate the observation departures from ARPEGE forecasts, as shown in Figure 5.

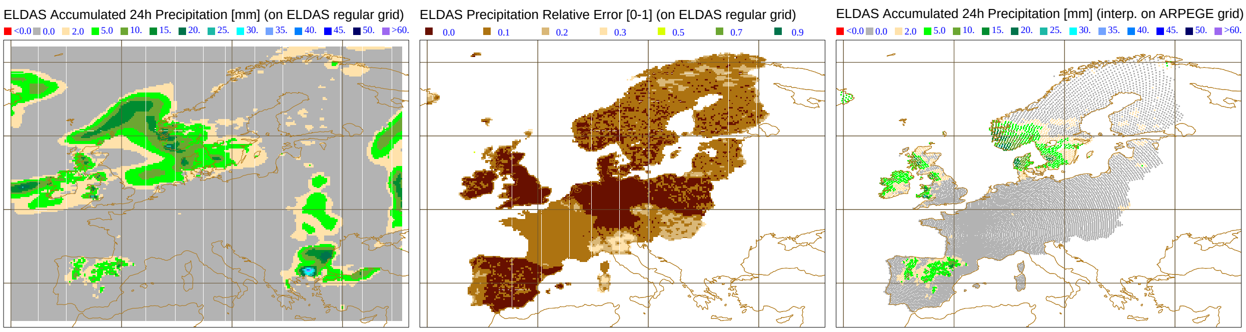

Figure 5: ELDAS precipitation forcing and its relative error (left and middle panels) for 2nd June 2000 and the ARPEGE interpolated forcing (right panel).

The correlation between 24-h accumulated precipitation (difference between 30-h and 6-h forecasts) and the total soil moisture is studied with the ARPEGE model to obtain a statistics and find out whether a linear relationship can be found. The correlation between precipitation amount and total soil moisture reservoir is expected to be high for significant rainfall events. The NMC statistics based on ARPEGE forecasts show an overall correlation of 0.89. The correlation increases with the precipitation amount (not shown), as soil water loss processes, such as evapotranspiration and drainage, become less effective in the evolution of soil moisture when large amount of precipitation occurs. To obtain an optimal (in a least square sense) coefficient $\alpha^P_{W\,p}$ for applying a total soil moisture increment (ΔW_p) based on the precipitation error (ΔP_{24h}) according to the following expression

$$\Delta W_p \;=\; \alpha^P_{W\,p}\Delta P_{24h} \qquad ; \qquad \left[\;\alpha^P_{W_p}\;\right] = \frac{\sigma^b_{W\,p}\sigma^b_{P_{24h}}\rho^b_{W_pP_{24h}}}{(\sigma^b_{P_{24h}})^2 + (\sigma^o_{P_{24h}})^2} \tag{9}$$

where the indices b and o stand for background and observation, respectively. In case of significant precipitation events, the following assumptions $\sigma^b_{W\,p} \simeq \sigma^b_{P_{24-h}}$ and $\sigma^b_{P_{24h}} \gg \sigma^o_{P_{24h}}$ are made, and the correlation $\rho^b_{W_pP_{24h}}$ previously calculated can be used to approximate such a coefficient. To better satisfy the above hypothesis on $\sigma^o_{P_{24h}}$, only grid points with a relative analysis error less than 0.5 are considered as valid observations. Since a 24-h accumulated precipitation forcing is available at 06 UTC and applies to the previous 24-h, a model background has to be extracted for the same accumulation period. For this purpose the forecast that transports the 2D-VAR analysis to the end of assimilation period is prolonged by 6-h (producing a 30-h forecast valid at 06 UTC at day+1) to calculate the accumulated precipitation. This choice has the advantage of providing a more

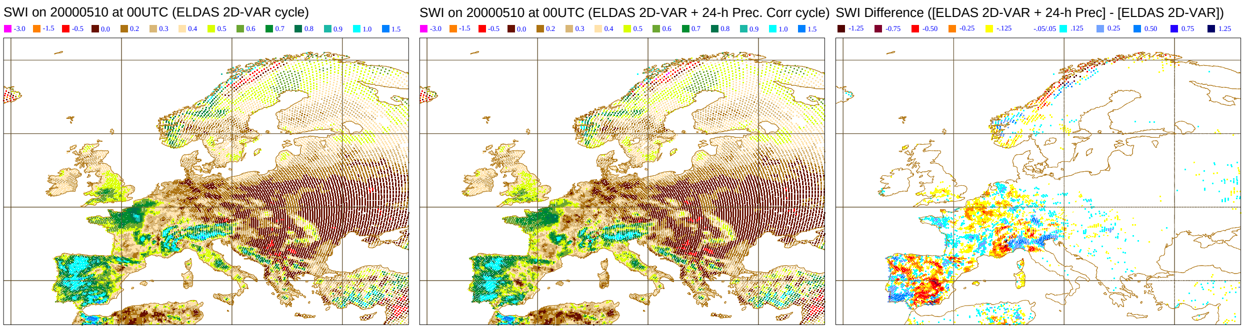

Figure 6: Soil Wetness Index (SWI) of the ELDAS assimilation cycle without (left panel) and with (middle panel) the use of precipitation forcing after 10 days, and their difference (right panel).

accurate background for the 24-h accumulated precipitation, since it is calculated between the 6-h forecast (with reduced spinup) and the 30-h forecast on a model trajectory already readjusted by the 2D-VAR analysis. The "2D-VAR + precipitation readjustments" and the "2D-VAR" cycles have been compared at the beginning of the ELDAS assimilation cycle in order to assess the impact of the ELDAS precipitation forcing on the total soil water content as is shown in Figure 6. The soil moisture fields resulting from the first 10 day assimilation cycles show the impact of the precipitation readjustment, which acts essentially to re-locate the precipitation amount (i.e. excess of precipitation forecasted over Iberian Peninsula) . The impact seems neutral elsewhere, with preservation of large scales in the soil moisture field in both experiments.

4 Model and assimilation description at MSC

4.1 A prototype for the Canadian Land Data Assimilation System

The Canadian Land Data Assimilation System (CaLDAS) is currently being developed at the Meteorological Service of Canada. A number of similarities concerning the land surface modelling and assimilation at the MSC and Météo-France has allowed us to benefit from the ELDAS experience. A land data assimilation prototype for the production of a global daily soil moisture analysis is built. The system is designed to receive different source of observations gathered from either ground-based and satellite instruments. The simplified variational (2D-VAR) technique is adapted in order to accomodate the observations at various times in a 24-h time-window, considering hour slots. The screen-level observations (temperature and humidity) are simulated together with presently available satellite observations, as for instance those provided by AQUA satellite (microwave C-band), GOES (infrared), and the observations to be provided in the future by HYDROS and SMOS satellite missions (microwave L-band). The introduction of a Canadian Precipitation Analysis (CaPA project, Mahfouf et al., 2004) will be investigated in the future to reduce the error of the background soil moisture field, by setting a complementary correction as previously described.

4.2 The land surface scheme

The land surface scheme ISBA (Noilhan and Planton, 1989) has been implemented operationally at the MSC together with the OI land surface analysis scheme (Mahfouf, 1991) as described in Bélair et al. (2003 I,II) and is currently used in the regional version of the Global Environmental Multiscale (GEM) model (Côté et al., 1998). Nevertheless in this study, the land surface simulation is done in an off-line mode where the land surface scheme is decoupled from the NWP model. The atmospheric forcing is provided at the lowest vertical level of the GEM model at an elevation of about 50m above the surface. This allows an interactive evolution of the surface boundary layer, without having to run the complete NWP model. The vertical interpolation is done according to Delage (1997) and provides the value at screen-level for temperature and humidity. The forcing frequency is 3-hourly.

4.3 The observation operator

To assimilate a new type of observations, a first step consists of implementing the corresponding observation operator. Microwave and infrared radiative transfer models for land surface already exist and have been tested in a number of experiments. In this study we have considered the Land Surface Microwave Emission Model (LSMEM), developed by Drusch et al. (1999, 2001) and the LMEB (L-band Microwave Emission of Biosphere) developed by Pellarin et al. (2003) for the micro-wave, and a simple approximation for the infra-red model. The LSMEM has been tested recently on several case studies (Seuffert et al. 2004, Gao et al. 2004, Drusch et al. 2004) and has been coupled to the ISBA scheme at MSC. The relationship between soil moisture and microwave brightness temperatures follows from the influence on the dielectric properties of the soil, and therefore on the emissivity. The solution of the radiative transfer equation is calculated according to Kerr and Njoku (1990). The vegetation contribution is treated according to the effective medium theory of Kirdyashev et al. (1979), and the vegetation opacity τ is made linearly dependent on the vegetation water content VWC and an experimental parameter b which accounts for the vegetation structure, according to the relationship

$$\tau = b \cdot VWC \tag{10}$$

The values of vegetation water content VWC, single scattering albedo w_*, and vegetation structure parameter b for the L-band are prescribed according to Pellarin et al. (2003) and readjusted (personal communications).

Class	w_* $(-)$	VWC $(kg \cdot m^{-2})$	$b(L-band)$ $(m^2 \cdot kg^{-1})$	$b(C-band)$ $(m^2 \cdot kg^{-1})$
grassland	0.04	0.5*LAI	0.1	0.5
crops	0.10	0.5*LAI	0.2	0.2
coniferous	0.10	3	0.1	0.5
broadleaf	0.10	4	0.1	0.5
tropical	0.10	6	0.1	0.5

Table 1: Microwave radiative transfer vegetation parameters: single scattering albedo (w_*), vegetation water content (VWC), and structure coefficient (b) for L-band and C-band.

Only few experimental observations are available to estimate the vegetation structure parameter and the values prescribed are probably subject to future revision. The clear-sky infrared skin temperature has been taken as the ISBA soil surface temperature (which accounts for a mixed soil-canopy temperature) over clear-sky area (with cloud cover fraction lower than 0.1). The approximation $T_s^{IR} \simeq T_s$ is equivalent to suppose a uniform infrared emissivity of 1.0 while in reality this value ranges between 0.95 and almost 1.0, depending on land surface physiography (and on the considered infrared channel). In a second step, a more realistic surface skin temperature and emissivity will be considered (Garand, 2003).

4.3.1 The temporal and spatial distribution of the observations

In order to build a realistic data assimilation prototype, the simulated observations have to be spatially and temporally distributed according to the prescribed satellite coverage. Table 2 reports a summary of orbital information to simulate the satellites overpasses and their views.

Satellite	Orbit Type	Altitude (km)	Inclination ($^\circ$)	Swath width (km)
HYDROS	sun-synchronous (6am,6pm e.q.t.)	670	98.0	1000
AQUA	sun-synchronous (1:30 pm e.q.t.)	705	98.2	1445
GOES E/W	Geostationary	36000	-	-

Table 2: Satellite orbital parameters: altitude, orbit description (e.q.t. is the equator crossing time), inclination, swath width.

The HYDROS polar orbit has been defined according to a Keplerian orbit (Larson and Wertz, 1992) which satisfies the prescribed satellite inclination, altitude and revisit time (Entekhabi et. al., 2004). The AQUA polar orbit has been taken from an observed satellite track. The geostationary satellite coverage has been simulated considering an elevation of 36000 km and a limit off-nadir angle of 8.0° to obtain the perimetral coverage as sketched in Figure 7. For the polar orbiting satellites, a circular swath with given amplitude around the nadir location has been considered to reproduce the expected satellite spatial coverage. Finally the simulated observations are stored in hourly slots considering the satellite's coverage along its trajectory between time $t_i = t - 30min.$ and $t_f = t + 30min.$ (as sketched in Figure 7). The infrared surface skin temperatures are generated only for morning hours when the relationship with soil moisture is more direct as in van den Hurk and The (2002). Each simulated observation is assumed to match perfectly the model gridbox and no subgrid information is considered.

4.4 The extension of the 2D-VAR formalism

In the CALDAS set up, the simplified 2D-VAR method makes use of the off-line driven land surface scheme coupled with the radiative transfer models to obtain the sensitivity of the observable Y to the analysis control variable (the total soil moisture W_p). The linearised observation operator $\mathbf{H}$ is calculated as $\Delta Y(t = t_i)/\Delta W_p(t = t_0)$, according to the perturbation method described in Balsamo et al. (2004) for the following observations: The L-band $T_{b,H}(L)$ and $T_{b,V}(L)$ (horizontal and vertical polarization at 1.4 GHz) and C-band $T_{b,H}(C)$ and $T_{b,V}(C)$ (6.9 GHz) brightness temperatures, the clear-sky infra-red skin temperature $T_s(IR)$, and the screen-level temperature T_{2m} and humidity Q_{2m}. Assuming all the simulated observations (one per type) are avalaible at different time in the assimilation time-window, the analysis for W_p is obtained as follow

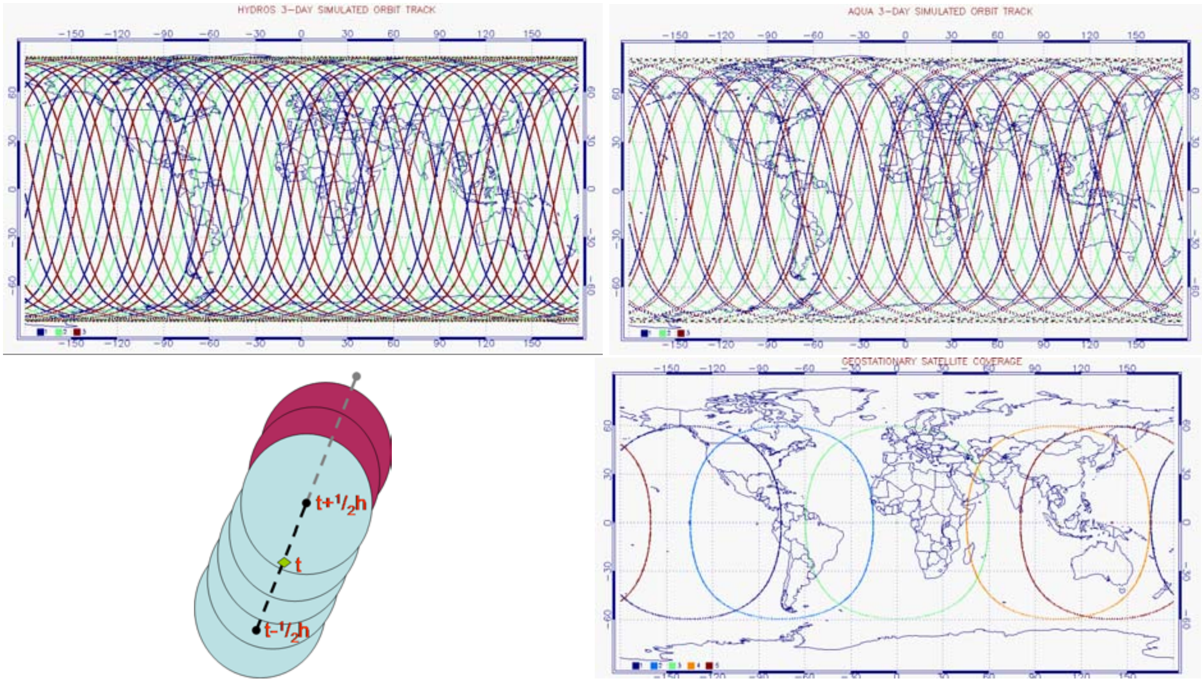

Figure 7: Satellite Observation Simulation: Upper panels show a 3-day polar satellite track orbit for HYDROS (left) and AQUA (right); the color indeces of the legend refer to the day (1 to 3). Bottom panels show the hourly observation sampling for polar orbiting satellites (left) and the geostationary global coverage (right) for (1) GOES EAST, (2) GOES WEST, (3) METEOSAT, (4) FENGYUN2, (5) GMS5.

$$W_p^a = W_p^b + \begin{pmatrix} k_1 & k_2 & k_3 & k_4 & k_5 & k_6 & k_7 \end{pmatrix} \begin{pmatrix} \Delta T_{b,H}(L)^{(1)} \\ \Delta T_{b,V}(L)^{(1)} \\ \Delta T_{b,H}(C)^{(2)} \\ \Delta T_{b,V}(C)^{(2)} \\ \Delta T_s(IR)^{(3)} \\ \Delta T_{2m}^{(4)} \\ \Delta Q_{2m}^{(4)} \end{pmatrix} \tag{11}$$

where the k_i terms are the elements of the analysis gain matrix **K** obtained from Eq. 4. The background error for soil moisture has been set to $\sigma_{W_p}^b$=10% $\cdot (w_{fc} - w_{wilt})$. The prescribed observation errors are given in Table 3.

Observation	σ^o
$T_b^{H,V}(L)$	3.0 K
$T_b^{H,V}(C)$	3.0 K
T_s^{IR}	3.0 K
T_{2m}	2.0 K
Q_{2m}	$2\ 10^{-3} \cdot kg \cdot kg^{-1}$

Table 3: Prescribed observation errors σ^o in the analysis.

The observation error covariance matrix **R** is a diagonal matrix composed of $(\sigma_Y^o)^2$ where the cross-covariances are neglected (the observation errors are supposed un-correleted).

5 The information content of the observations in the analysis

The diagnostic $Trace(\mathbf{HK})$ as described in Cardinali et al. (2003), can be used to infer the weight of an observation type in the analysis. If the observation operator **H** is applied on both sides of the analysis equation (Eq. 4) then:

$$\mathbf{Hx}^a = \mathbf{Hx}^b + \mathbf{HK}(\mathbf{y} - H(\mathbf{x}^b)) \tag{12}$$

Differentiating the above equation with respect to the observation $\mathbf{y}_0$ and taking the trace of the resulting matrix gives the sensitivity of the analysis to a given observation type:

$$Tr(\frac{\partial \mathbf{Hx}^a}{\partial \mathbf{y}_0}) = Tr(\mathbf{HK}) \tag{13}$$

which when **H** is linear corresponds to the analysis error reduction, so that

$$Tr(\mathbf{HK}) = Tr((\mathbf{B} - \mathbf{A})\mathbf{B}^{-1}) \tag{14}$$

where **A** and **B** are the error covariance matrices for the analysis and the background, respectively. This diagnostic is used to estimate the relative information content of the each observation type in the soil moisture analysis.

5.1 The OSSE experiment

An Observing System Simulation Experiment (OSSE) is set up to test the performance of the analysis and investigate the impact of each assimilated observation type in correcting a given soil moisture initial error. A simplified 2D-VAR assimilation experiment with a 24-h time-window is performed over North America (domain latitude $[28,73]$ and longitude $[228,305]$) at a resolution of $0.5°$ on 5th July 2004. The assimilated observations are simulated according to the procedure described, and a sample is provided in Figure8. The

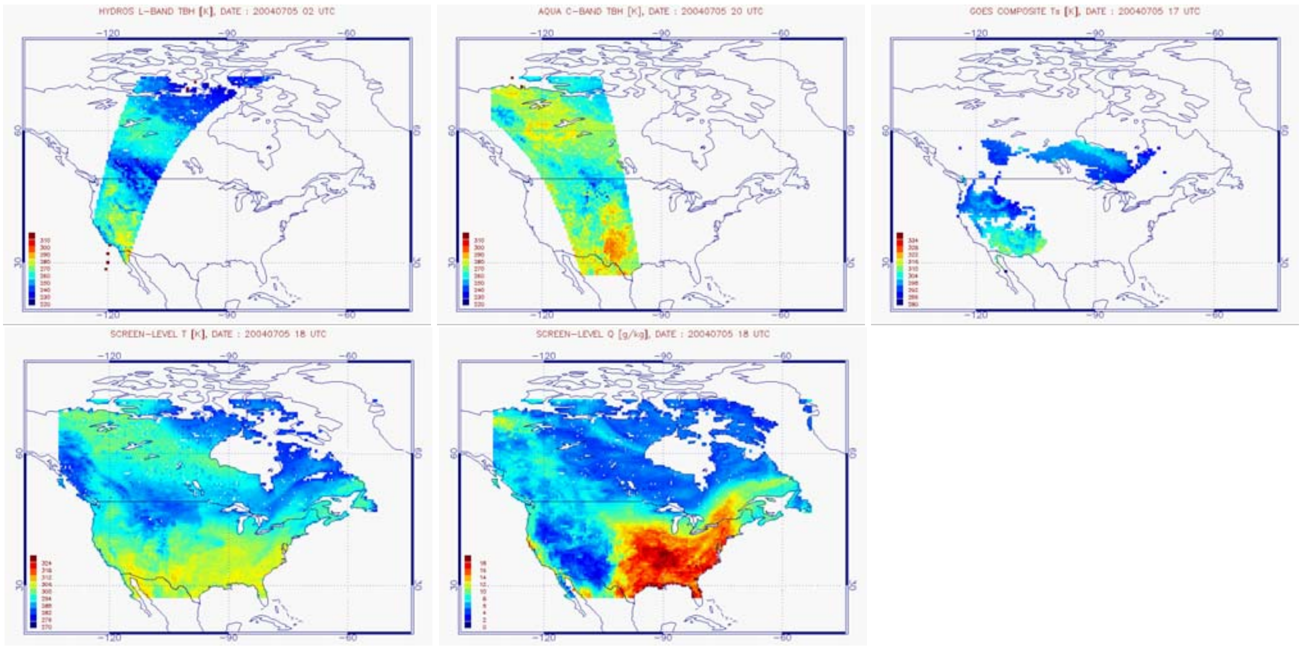

Figure 8: Examples of simulated observations for 5th July 2004 (from top left panel): $T_b^H(L)$, $T_b^H(C)$, T_s^{IR}, T_{2m}, Q_{2m}.

objective of this test is to assess the impact of the simulated observations on the soil moisture analysis. This type of experiment is similar to the one performed for the analysis convergence. The results of an assimilation cycle are analysed for producing the $Tr(\mathbf{HK})$ diagnostic, summarized in Figure9. In this case about 36% of

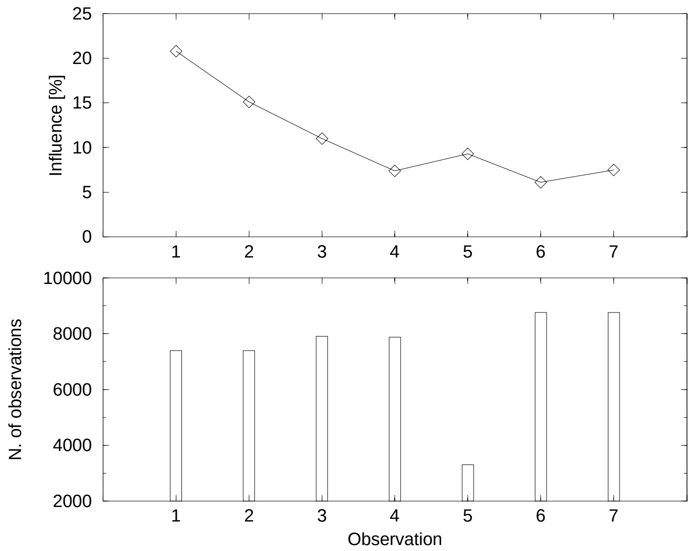

Figure 9: Influence of the observation in the analysis (top) and number of observations (bottom). The observations are (1) $T_b^H(L)$, (2) $T_b^V(L)$, (3) $T_b^H(C)$, (4) $T_b^V(C)$, (5) T_s^{IR}, (6) T_{2m}, (7) Q_{2m}.

the analysis influence is provided by the L-band observations, 18% by the C-band, 13% by the screen-level, and 9% by the infrared. If these results are normalizes by the number of observations, the infrared surface temperature has a larger contribution (about 24%) but this value is likely to change from one day to another according to the cloud cover conditions. A similar remark can be made for the screen-level observations since the soil moisture sensitivity is bounded between the soil wilting point and the field capacity, and reduced under specific meteorological and land surface conditions. From these results, the influence of the observations in the analysis appears to be proportional to the ratio given by the dynamical range of the observable Y divided by the observation error σ^o.

6 Conclusions

A linearised variational technique for the analysis of total soil water content via the assimilation of screen-level observations has been implemented and evaluated in both the ALADIN Mesoscale NWP model and the ARPEGE GCM model with a 24-h assimilation time-window. Simulated and real observations experiments with ALADIN (Balsamo et al., 2004), where the new soil moisture initialization is applied, have lead to an improvement of the 72-h forecast scores combined with a more realistic soil moisture field. The application within the European Land Data Assimilation System (ELDAS project, van den Hurk, 2002), has required the use of a larger integration domain. The 2D-VAR has been implemented in the context of the the global stretched GCM model ARPEGE for the production of a global daily soil moisture analysis. The stretched grid geometry allows a fine resolution over the ELDAS domain. The ELDAS precipitation analysis has been considered via an off-line correction to the soil moisture applied sequentially at the end of the daily 2D-VAR analysis. This complementary correction allows one to account for the non-Gaussian behaviour of precipitation errors. The 2D-VAR can not immediately correct these errors because the evapotranspiration signature (present in the assimilated 2m observations) is reduced or negligible. The hydrological consistency has been checked by comparing the analysis to the output produced by the ISBA-MODCOU system over France (Habets et al., 1999 I,II).
A prototype of the Canadian Land Data Assimilation System (CaLDAS) has been implemented at MSC from ELDAS experience. CaLDAS has been used to extend the data assimilation technique to other relevant observations. The ISBA land surface scheme integration is realized in off-line mode, where the atmospheric forcing is provided by the lowest NWP model level at 50 m above the ground, preserving an interactive surface boundary layer. The influence matrix diagnostic (Cardinali et al., 2003) has been implemented for this assimilation

system to study the relative contribution of each observation type assimilated in the analysis. The experiment using "perfect observations" allows an objective evaluation of the importance of a given observation type on the land surface analysis. Preliminary results show a large contribution of microwave brightness temperatures and in particular of the L-band as theoretically expected. These observations have the advantage of a reduced atmospheric absorption and a wide dynamical range. The associated information content is likely to remain stable. Infrared skin temperature observations represent a significant source of information especially considering the observation frequency, but the temporal and spatial availability is strongly variable and shows a latitude dependence (van den Hurk and The, 2002). The screen-level observations are informative on the evapotranspiration processes and their information content may vary. Although it is not the dominant data source, these variables would probably prevent drifts produced by atmospheric feedbacks in case of an erroneous representation of the land surface, which is high priority for NWP purposes. Conclusions should be balanced with practical considerations on the current difficulties associated with the use of satellite information over land. The above methodology can be a useful tool for evaluating the land data assimilation system. Real observations experiments will be considered in the near future to evaluate the assimilation and assess the generality of the present conclusions.

Acknowledgements

The authors wish to thank the ELDAS science team (co-ordinator B. van den Hurk) and the HYDROS science team (P.I. D. Entekhabi). The research activity has been supported by EU-Project ALATNET (ALAdin Training NETwork, co-ordinator J.-F. Geleyn), the French CNRS (National Centre of Scientific Research), the Canadian NSERC (National Science and Engineering Council of Canada) and the CSA (Canadian Space Agency). Acknowledgements go to the ALADIN and HIRLAM working groups on soil and surface analyses for their interest and precious advice on the subject and to RPN and ARMA teams.

References

Balsamo G., Bouyssel F., Noilhan J. (2004) A simplified bi-dimensional variational analysis of soil moisture from screen-level observations in a mesoscale numerical weather prediction model. *Q. J. R. Met. Soc.* **130A, 598**, 895-916

Bélair S., Brown R., Mailhot J., Bilodeau B. and Delage Y. (2003) Operational Implementation of the ISBA land surface scheme in the Canadian regional weather forecast model. Part I: Warm season results. *J. Hydromet.* **4,** 352-370

Bélair S., Brown R., Mailhot J., Bilodeau B. and Crevier L.-P. (2003) Operational Implementation of the ISBA land surface scheme in the Canadian regional weather forecast model. Part II: Cold season results. *J. Hydromet.* **4,** 371-386.

Boone A., Calvet J.C., Noilhan J. 1999 Inclusion of a third soil layer in a land-surface scheme using the force restore method. *J. Appl. Meteorol.* **38,** 1611-1630.

Boone A. and Etchevers P. (2001) An intercomparison of three snow schemes of varying complexity coupled to the same land-surface and macroscale hyrologic model. *J. Hydromet.* **2,** No. 4, 374-394.

Bouyssel F., Cassé V. and Pailleux J. (2000) Variational surface analysis from screen-level atmospheric parameters. *Tellus* **51A,** 453-468.

Bouttier F., Mahfouf J.F, Noilhan J. 1993 Sequential assimilation of soil moisture from atmospheric low-level parameters. PART I: Sensitivity and calibration studies. *J. Appl. Meteorol.* **32,** 1335-1351.

Bouttier F., Mahfouf J.F, Noilhan J. 1993 Sequential assimilation of soil moisture from atmospheric low-level parameters. PART II : Implementation in a mesoscale model. *J. Appl. Meteorol.* **33,** 1352-1364.

Bubnová R., A. Horanyi, and S. Malardel 1993 International project ARPEGE/ALADIN. *EWGLAM Newsl.* **22,** 117-130.

Callies U. and Rhodin A. and Eppel D.P. 1998 A case study on variational soil moisture analysis from atmospheric observations. *J. Hydrol.* **212-213,** 95-108.

Calvet J.C. 1998 An interactive vegetation model tested against data from six contrasting sites. *Agric. Forest Meteorol.* **2564,** 1-23.

Cardinali C., Pezzulli S. and Andersson E. (2003) Influence matrix diagnostic of a data assimilation system. *ECMWF Seminar on Recent developments in data assimilation for atmospheric and ocean, 8-13 September.*

Côté J., Gravel S., Méthot A., Patoine A., Roch M and Staniforth A. (1998) The operational CMC-MRB Global Environmental Multiscale (GEM) model: part I - design considerations and formulation. *Mon. Wea. Rev.,* **126,** 1373-1395.

Courtier P., Freydier C., Geleyn J.F., Rabier F., and Rochas M. (1991) The ARPEGE project at Météo-France. *Proc. ECMWF Seminar* **2,** 193-232.

Delage Y. (1997) Parametrizing sub-grid scale vertical transport in atmospheric models under statically stable conditions. *Bound. Layer Meteorol.* **82,** 23-48.

Drusch M., Wood E. F., and Simmer C. (1999) Up-scaling effects in passive microwave remote sensing: ESTAR 1.4 GHz measurements during SGP97. *Geophys. Res. Lett.* **26,** 879-882.

Drusch M., Wood E. F., Jackson T. (2001) Vegetative and atmospheric corrections for soil moisture retrieval from passive microwave remote sensing data Results from the Southern Great Plains hydrologic experiment 1997. *J. Hydromet.* **2,** 181-192.

Drusch M., Wood E., Gao H., and Thiele A. (2004) Soil moisture retrieval during the Southern Great Plains Hydrology Experiment 1999: A comparison between experimental remote sensing data and operational products. *Water Resour. Res.* **40,** W02504, doi:10.1029/2003WR002441.

Entekhabi D., Njoku E., Houser P., Spencer M., Doiron T., Smith T., Girard R., Bélair S., Crow W., Jackson T., Kerr Y., Kimball J., Koster R., McDonald K., O'Neill P., Pultz T., Running S., Shi J.C., Wood E., van Zyl J. (2004) The Hydrosphere State (HYDROS) Mission Concept: An Earth System Pathfinder for Global Mapping of Soil Moisture and Land Freeze/Thaw. *IGARS special issue*

Gao H., Wood E. F., Drusch M., Crow W. and Jackson T. (2004) Using a microwave emission model to estimate soil moisture from ESTAR observations during SGP99. *J. Hydromet.* **5,** 49-63.

Garand L. (2003) Towards an integrated land-ocean surface skin temperature analysis from the variational assimilation of infrared radiances. *J. Appl. Meteorol.* **42,** 570-583.

Geleyn J.F. (1988) Interpolation of wind, temperature, humidity values from model levels to the height of measurement. *Tellus* **40A,** 347-351.

Geleyn J.F., Bazile E., Bougeault P., Déqué M., Ivanovici V. Joly A., Labbé L. Piédelievre J.P., Piriou J.M. and Royer J.F. (1995) Atmospheric parameterization scheme in Météo-France's ARPEGE N.W.P. *Proc. of the 1994 ECMWF Seminar on Physical parameterizations in numerical models* 385-402, Reading.

Giard D. and Bazile E. (2000) Implementation of a new assimilation scheme for soil and surface variables in a global NWP model. *Mon. Wea. Rev.* **128,** 997-1015.

Guidard V. and Fischer C. (2003) Combined use of 3d-var and DFI-blending on MAP IOP 14. *ALADIN/ALATNET Newsletter n. 22/5*

Habets F., Noilhan J., Golaz C., Goutorbe J.P., Lacarrére P., Leblois E., Ledoux E., Martin E., Ottlé C., Vidal-Madjar D. (1999) The ISBA surface scheme in a macroscale hydrological model applied to the Hapex-Mobilhy area. Part I: Model and database. *J. Hydrol.* **1-2,** 75-96.

Habets F., Noilhan J., Golaz C., Goutorbe J.P., Lacarrére P., Leblois E., Ledoux E., Martin E., Ottlé C., Vidal-Madjar D. (1999) The ISBA surface scheme in a macroscale hydrological model applied to the Hapex-Mobilhy area. Part II: Simulation of streamflow and annual water budget. *J. Hydrol.* **1-2,** 97-118.

Hess R. (2001) Assimilation of screen-level observations by variational soil moisture analysis. *Meteorol. Atmos. Phys.* **77,** 145-154.

van den Hurk B. (2002) European LDAS established. *GEWEX Newsletter* **12,** 9.

Van den Hurk, B. and H. The (2002) Assimilation of satellite derived surface heating rates in a Numerical Weather Prediction Model. *KNMI Scientific Report* **WR 2002-04.**

Janisková M., Thépaut J.N., Geleyn J.F. (1999) Simplified and regular physical parametrizations for incremental four-dimensional variational assimilation. *Mon. Wea. Rev.* **127,** 26-45.

Kerr, Y.H., Waldteufel P., Wigneron J.-P., Font J., Berger M. (2001) Soil moisture retrieval from space: The Soil Moisture and Ocean Salinity (SMOS) mission. *IEEE Trans. Geosci. Remote Sens.* **39,** 1729-1735.

Kerr Y. and Njoku E. (1990) A semiempirical model for interpreting microwave emission from semiarid land surfaces as seen from space. *IEEE Trans. Geosc. Remote Sens.* **28,** 384-393.

Kirdyashev K., Chukhlantsev A., Shutko A. (1979) Microwave radiation of the Earths surface in the presence of a vegetation cover. *Radio Eng. Electron. Phys.* **24,** 37-44.

Koster R., Dirmeyer P., and the GLACE team (2004) Regions of strong coupling between soil moisture and precipitation. *Science* **305,** 1138-1140.

Larson, W. J. and J. R. Wertz (1992) Space Mission Analysis and Design. *Kluwer, Netherlands.*

Louis J.F. (1979) A parametric model of vertical eddy fluxes in the atmosphere. *Boundary-Layer Meteorol.* **17,** 187-202.

Louis J.F., Tiedtke M. and Geleyn J.F. (1981) A short history of the operational PBL parameterization at ECMWF. *Workshop on the Planetary boundary layer parameterization.* 59-80, Reading, 25-27 November.

Mahfouf J.-F. (1991) Analysis of soil moisture from near-surface parameters: A feasibility study. *J. Appl. Meteorol.* **30,** 1534-1547.

Mahfouf J.-F., Viterbo P., Douville H., Beljaars A.C.M. and Saarinen S. (2000) A revised land-surface analysis scheme in the Integrated Forecasting System. *ECMWF Newsletter* **88,** 8-13.

Mahfouf J.-F., Brasnett B., Gagnon S. (2004) Description of the Canadian Precipitation Analysis (CaPA) project. *available from MSC, MRB/RPN Canada.*

Masson, V., Champeaux, J.-L., Chauvin, F., Meriguet, C. and Lacaze, R. (2003) A global database of Land Surface Parameters at 1-km Resolution in Meteorological and Climate Models. *J. Climate* **16,** 9, 1261-1282.

Noilhan J., Planton S. (1989) A simple parameterization of land surface processes for meteorological models. *Mon. Wea. Rev.* **117,** 536-549.

Noilhan J., Mahfouf J.-F. (1996) The ISBA land surface parameterization scheme. *Global and Planetary Change* **16,** 145-159.

Pellarin T., Calvet J.-C., Wigneron J.-P. (2003) Surface soil moisture retrieval from L-band radiometry: a global regression study. *IEEE Trans. Geosc. Remote Sens.* **41,** 2135-2139.

Rhodin A., Kucharski F., Callies U., Eppel D.P. (1999) Variational soil moisture analysis from screen-level atmospheric parameters: Application to a short-range weather forecast model. *Q. J. R. Met. Soc.* **125,** 2427-2448.

Rubel F., Skomorowski P. and Brugger K. (2004) A new 3-hourly precipitation dataset for NWP model verification and data assimilation studies. *4th Study Conf. on BALTEX, Gudhjem, Bornholm, Denmark. 24-28 May.*

Seuffert, G., Wilker, H., Viterbo, P., Drusch, M., Mahfouf, J.-F. (2004) The usage of screen-level parameters and microwave brightness temperature for soil moisture analysis. *J. Hydromet.,* **5**, 3, 516-531.